E1-2004-87

MEASUREMENTS OF THE TOTAL CROSS-SECTION DIFFERENCE $\Delta\sigma_L(np)$ AT 1.39, 1.69, 1.89 AND 1.99 GeV

Submitted to «Ядерная физика»

V. I. Sharov[1,*], N. G. Anischenko[1], V. G. Antonenko[2], S. A. Averichev[1], L. S. Azhgirey[3], V. D. Bartenev[1], N. A. Bazhanov[3], A. A. Belyaev[5], N. A. Blinov[1], N. S. Borisov[3], S. B. Borzakov[6], Yu. T. Borzunov[1], Yu. P. Bushuev[1], L. P. Chernenko[6], E. V. Chernykh[1], V. F. Chumakov[1], S. A. Dolgii[1], A. N. Fedorov[3], V. V. Fimushkin[1], M. Finger[3,7], M. Finger, Jr.[3], L. B. Golovanov[1], G. M. Gurevich[8], A. Janata[3], A. D. Kirillov[1], V. G. Kolomiets[3], E. V. Komogorov[1], A. D. Kovalenko[1], A. I. Kovalev[4], V. A. Krasnov[1], P. Krstonoshich[3], E. S. Kuzmin[3], V. P. Ladygin[1], A. B. Lazarev[3], F. Lehar[9], A. de Lesquen[9], M. Yu. Liburg[1], A. N. Livanov[1], A. A. Lukhanin[5], P. K. Maniakov[1], V. N. Matafonov[3], E. A. Matyushevsky[1], V. D. Moroz[1], A. A. Morozov[1], A. B. Neganov[3], G. P. Nikolaevsky[1], A. A. Nomofilov[1], Tz. Panteleev[6,10], Yu. K. Pilipenko[1], I. L. Pisarev[3], Yu. A. Plis[3], Yu. P. Polunin[2], A. N. Prokofiev[4], V. Yu. Prytkov[1], P. A. Rukoyatkin[1], V. A. Schedrov[4], O. N. Schevelev[3], S. N. Shilov[3], R. A. Shindin[1], M. Slunečka[3,7], V. Slunečková[3], A. Yu. Starikov[1], G. D. Stoletov[3], L. N. Strunov[1], A. L. Svetov[1], Yu. A. Usov[3], T. Vasiliev[1], V. I. Volkov[1], E. I. Vorobiev[1], I. P. Yudin[11], I. V. Zaitsev[1], A. A. Zhdanov[4], V. N. Zhmyrov[3]

---

[1]Joint Institute for Nuclear Research, Veksler and Baldin Laboratory of High Energies, 141980 Dubna, Russia

[*]E-mail: sharov@sunhe.jinr.ru

[2]Russian Scientific Center «Kurchatov Institute», 123182 Moscow, Russia

[3]Joint Institute for Nuclear Research, Dzhelepov Laboratory of Nuclear Problems, 141980 Dubna, Russia

[4]St. Petersburg Nuclear Physics Institute, High Energy Physics Division, 188350 Gatchina, Russia

[5]Kharkov Institute of Physics and Technology, 310108 Kharkov, Ukraine

[6]Joint Institute for Nuclear Research, Frank Laboratory of Neutron Physics, 141980 Dubna, Russia

[7]Charles University, Faculty of Mathematics and Physics, V Holešovičkách 2, 180 00 Praha 8, Czech Republic

[8]Institute for Nuclear Research, Russian Academy of Sciences, 117312 Moscow, Russia

[9]DAPNIA, CEA/Saclay, 91191 Gif-sur-Yvette Cedex, France

[10]Institute for Nuclear Research and Nuclear Energy, Bulgarian Academy of Sciences, 1784 Sofia, Bulgaria

[11]Joint Institute for Nuclear Research, Laboratory of Particle Physics, 141980 Dubna, Russia

Шаров В. И. и др. E1-2004-87

Измерения разности полных сечений $\Delta\sigma_{\mathrm{L}}(np)$
при энергиях 1,39; 1,69; 1,89 и 1,99 ГэВ

Представлены новые точные результаты измерений спин-зависимой разности полных нейтрон-протонных сечений $\Delta\sigma_{\mathrm{L}}(np)$ при кинетических энергиях нейтронов 1,39; 1,69; 1,89 и 1,99 ГэВ. В основном, эти данные завершают измерения энергетической зависимости $\Delta\sigma_{\mathrm{L}}(np)$ в области энергий дубненского синхрофазотрона. Почти монохроматический нейтронный пучок получался при развале выведенных из синхрофазотрона векторно-поляризованных дейтронов. Знак поляризации дейтронов (а следовательно, и нейтронов) менялся от цикла к циклу. Вертикальная ориентация поляризации нейтронов поворачивалась по направлению нейтронного пучка, и продольно-поляризованные нейтроны пропускались через большую продольно-поляризованную протонную мишень. Направление продольной поляризации мишени инвертировалось спустя 1–2 сут измерений. Быстрый спад $-\Delta\sigma_{\mathrm{L}}(np)$ с ростом энергии выше 1,1 ГэВ и структура в энергетической зависимости вокруг 1,8 ГэВ, впервые наблюденные в более ранних измерениях, кажутся явно выраженными. Новые данные сравниваются с модельными предсказаниями и с решениями фазового анализа. Приводятся значения $\Delta\sigma_{\mathrm{L}}$ для изосинглетного состояния $I=0$, полученные из измеренных $\Delta\sigma_{\mathrm{L}}(np)$-величин и известных $\Delta\sigma_{\mathrm{L}}(pp)$-данных. Представлены также результаты измерений полных np- и nC-сечений при нескольких энергиях, полученные с использованием той же установки на высокоинтенсивных пучках неполяризованных дейтронов, выводимых либо из синхрофазотрона, либо из нуклотрона.

Работа выполнена в Лаборатории высоких энергий им. В. И. Векслера и А. М. Балдина ОИЯИ.

Препринт Объединенного института ядерных исследований. Дубна, 2004

Sharov V. I. et al. E1-2004-87

Measurements of the Total Cross-Section Difference $\Delta\sigma_{\mathrm{L}}(np)$
at 1.39, 1.69, 1.89 and 1.99 GeV

New accurate results of the neutron–proton spin-dependent total cross-section difference $\Delta\sigma_{L}(np)$ at the neutron beam kinetic energies of 1.39, 1.69, 1.89 and 1.99 GeV are presented. In general these data complete the measurements of energy dependence of $\Delta\sigma_{\mathrm{L}}(np)$ over the Dubna Synchrophasotron energy region. The quasi-monochromatic neutron beam was produced by break-up of extracted polarized deuterons. The deuteron (and hence neutron) polarization direction was flipped every accelerator burst. The neutron vertical direction of polarization was rotated onto the neutron beam direction and longitudinally (L) polarized neutrons were transmitted through the large proton L-polarized target. The longitudinal target polarization direction was inverted after 1–2 days of measurements. Four different combinations of the beam and target parallel and antiparallel polarization directions, both oriented along the neutron beam momentum, were used at each energy. A fast decrease of $-\Delta\sigma_{\mathrm{L}}(np)$ with increasing energy above 1.1 GeV and a structure in the energy dependence around 1.8 GeV, first observed from our previous data, seem to be well revealed. The new results are also compared with model predictions and with phase shift analysis fits. The $\Delta\sigma_{\mathrm{L}}$ quantities for isosinglet state $I=0$, deduced from the measured $\Delta\sigma_{\mathrm{L}}(np)$ values and known $\Delta\sigma_{\mathrm{L}}(pp)$ data, are also given. The results of the measurements of unpolarized total cross sections $\sigma_{0\mathrm{tot}}(np)$ at 1.3, 1.4 and 1.5 GeV and $\sigma_{0\mathrm{tot}}(nC)$ at 1.4 and 1.5 GeV are presented as well. These data were obtained using the same apparatus and high intensity unpolarized deuteron beams extracted either from the Synchrophasotron, or from the Nuclotron.

The investigation has been performed at the Veksler and Baldin Laboratory of High Energies, JINR.

Preprint of the Joint Institute for Nuclear Research. Dubna, 2004

INTRODUCTION

The paper presents new results of the spin-dependent neutron-proton total cross-section difference $\Delta\sigma_{\rm L}(np)$, measured in 2001 with a quasi-monochromatic polarized neutron beam and the polarized proton target (PPT). The $\Delta\sigma_{\rm L}(np)$ values were obtained at neutron beam kinetic energies of 1.39, 1.69, 1.89, and 1.99 GeV.

The free polarized neutron beam with a sufficient intensity was produced by break-up of polarized deuterons accelerated by the Synchrophasotron of the Veksler and Baldin Laboratory of High Energies (JINR, Dubna). This accelerator provides the highest energy (3.7 GeV) polarized neutron beam that can be reached at the present moment.

The spin-dependent NN-observables $\Delta\sigma_{\rm L}$ and $\Delta\sigma_{\rm T}$ are defined as a difference in the NN total cross sections for the antiparallel and parallel beam and target polarizations, oriented longitudinally (L) and transverse (T) to the beam direction. Transmission measurements of the $\Delta\sigma_{\rm L}(np)$ and $\Delta\sigma_{\rm T}(np)$ energy dependences over the Synchrophasotron neutron beam energy range of 1.2–3.7 GeV, have been proposed [1, 2] and started [3, 4, 5, 6] in Dubna. The measurements were carried out within the program of the JINR project «DELTA–SIGMA experiment». The aim of this experimental program is to obtain sufficient data set on the np polarization observables over this new highest energy region of free polarized neutron beams and to do a direct reconstruction of the imaginary and real parts of the spin-dependent forward scattering np amplitudes for the first time.

To carry out $\Delta\sigma_{\rm L}(np)$ measurements, a large Argonne–Saclay polarized proton target (PPT) was reconstructed at Dubna [7–9] and a new polarized neutron beam line [10, 11] with suitable parameters was made and tested. A set of dedicated neutron detectors with corresponding electronics was used. The data acquisition system was based on CAMAC parallel branch highway controlled by IBM PC with the branch driver [12] finished off by one of the authors. On-line program in Pascal works under DOS. The successful data taking runs were carried out in 1995 and 1997 and the $\Delta\sigma_{\rm L}(np)$ values were measured at 1.19, 1.59, 1.79, 2.20, 2.49, and 3.66 GeV [2–6]. For the measurements in 1997, a new PPT polarizing solenoid [13] was developed at VBLHE.

The nucleon–nucleon (NN) total cross-section differences $\Delta\sigma_{\rm L}$ and $\Delta\sigma_{\rm T}$, together with the spin-average total cross section $\sigma_{0\rm tot}$, were measured in pure inclusive transmission experiments. They were linearly related with three non-vanishing imaginary parts of the NN forward scattering amplitudes via optical

theorems and allowed one to reconstruct directly these imaginary parts. The data were also used to check the predictions of available dynamic models and to provide an important contribution to databases of phase-shift analyses (PSA). From the measured $\Delta\sigma_{\rm L}(np)$ values it was possible to deduce the $\Delta\sigma_{\rm L}$ nucleon–nucleon isosinglet ($I = 0$) part, using the existing pp (isotriplet $I = 1$) results.

The total cross-section differences $\Delta\sigma_{\rm L,T}$ for pp scattering were first measured at the ANL–ZGS and then at TRIUMF, in PSI, at LAMPF, SATURNE II and in Fermilab. Results were obtained in the energy range from 0.2 to 12 GeV and at 200 GeV. Measurements with incident charged particles need an experimental set-up different from neutron–proton experiments, due to the contribution of electromagnetic interactions. Existing $\Delta\sigma_{\rm L,T}(pp)$ results are discussed in [14] and in references therein.

$\Delta\sigma_{\rm L}(pn)$ results from 0.51 to 5.1 GeV were deduced for the first time in 1981 from the $\Delta\sigma_{\rm L}(pd)$ and $\Delta\sigma_{\rm L}(pp)$ measurements at the ANL–ZGS [15]. These pn results were omitted in many existing PSA databases due to uncertainties in the Glauber-type rescattering corrections. They were discussed in [3, 4, 14].

Using free polarized neutrons at Saturne II, $\Delta\sigma_{\rm T}(np)$ and $\Delta\sigma_{\rm L}(np)$ results were obtained at 11 and 10 values of energy in the range from 0.31 to 1.10 GeV, respectively [16, 17, 18]. The Saclay results were soon followed by PSI measurements [19] at seven energy bins from 0.180 to 0.537 GeV, using a continuous neutron energy spectrum. The PSI and Saclay sets allowed one to deduce imaginary parts of np and $I = 0$ spin-dependent forward scattering amplitudes [14, 18]. Only $\Delta\sigma_{\rm L}(np)$ was measured at five energies between 0.484 and 0.788 GeV at LAMPF [20]. A quasi-monoenergetic polarized neutron beam was produced in $pd \Rightarrow n + X$ scattering of longitudinally polarized protons.

At low energies, $\Delta\sigma_{\rm L}(np)$ was measured at 66 MeV at the PSI injector [21], and at 16.2 MeV in Prague [22]. $\Delta\sigma_{\rm T}(np)$ was determined in TUNL at nine energies between 3.65 and 11.6 MeV [23], and at 16.2 MeV in Prague [24]. Recently the TUNL measured $\Delta\sigma_{\rm L}(np)$ at six energies between 4.98 and 19.7 MeV [25] and $\Delta\sigma_{\rm T}(np)$ at three other energies between 10.7 and 17.1 MeV [26].

At high energies the $\Delta\sigma_{\rm L}(np)$ results using free polarized neutrons were obtained at the JINR Synchrophasotron only. The Dubna results smoothly connect with the existing data at lower energies. The $-\Delta\sigma_{\rm L}(np)$ energy dependence shows a fast decrease to zero above 1.1 GeV and a structure around 1.8 GeV. Values of the $I = 0$ part of $\Delta\sigma_{\rm L}$ are also presented. The data are compared with model predictions and the PSA fits.

Section 1 gives a brief determination of observables. Section 2 describes the method of measurements. The essential details concerning the beam, the polarimeters, the experimental set-up and PPT are given in Sec. 3. Data acquisition and analyses are described in Sec. 4. Results and discussion are presented in Sec. 5.

1. DETERMINATION OF OBSERVABLES

Throughout this paper we use the NN formalism and notations for elastic nucleon–nucleon scattering observables from [27].

The general expression of the total cross section for a polarized nucleon beam transmitted through the PPT, with arbitrary directions of the beam and target polarizations, $\mathbf{P}_{\rm B}$ and $\mathbf{P}_{\rm T}$, respectively, was first deduced in Refs. [28, 29]. Taking into account fundamental conservation laws, it is written in the form:

$$\sigma_{\rm tot} = \sigma_{0\rm tot} + \sigma_{1\rm tot}(\mathbf{P}_{\rm B}, \mathbf{P}_{\rm T}) + \sigma_{2\rm tot}(\mathbf{P}_{\rm B}, \mathbf{k})(\mathbf{P}_{\rm T}, \mathbf{k}), \tag{1.1}$$

where $\mathbf{k}$ is a unit vector in the direction of the beam momentum. The term $\sigma_{0\rm tot}$ is the total cross section for unpolarized particles, $\sigma_{1\rm tot}$, $\sigma_{2\rm tot}$ are the spin–dependent contributions. They are related to the measurable observables $\Delta\sigma_{\rm T}$ and $\Delta\sigma_{\rm L}$ by

$$-\Delta\sigma_{\rm T} = 2\sigma_{1\rm tot}, \tag{1.2}$$

$$-\Delta\sigma_{\rm L} = 2(\sigma_{1\rm tot} + \sigma_{2\rm tot}), \tag{1.3}$$

called «total cross-section differences». The negative signs for $\Delta\sigma_{\rm T}$ and $\Delta\sigma_{\rm L}$ in Eqs. (2.2) and (2.3) correspond to the usual, although unjustified, convention in the literature. The total cross-section differences are measured with either parallel or antiparallel beam and target polarization directions. Polarization vectors are transversally oriented with respect to $\mathbf{k}$ for $\Delta\sigma_{\rm T}$ measurements and longitudinally oriented for $\Delta\sigma_{\rm L}$ experiments. Only $\Delta\sigma_{\rm L}$ measurements are treated below, but the formulae are similar for the both total cross-section differences.

For $\mathbf{P}_{\rm B}^{\pm}$ and $\mathbf{P}_{\rm T}^{\pm}$, all oriented along $\mathbf{k}$, we obtain four total cross sections:

$$\sigma(\rightrightarrows) = \sigma(++) = \sigma_{0\rm tot} + |{\rm P}_{\rm B}^{+}{\rm P}_{\rm T}^{+}|\ (\sigma_{1\rm tot} + \sigma_{2\rm tot}), \tag{1.4a}$$

$$\sigma(\leftrightarrows) = \sigma(-+) = \sigma_{0\rm tot} - |{\rm P}_{\rm B}^{-}{\rm P}_{\rm T}^{+}|\ (\sigma_{1\rm tot} + \sigma_{2\rm tot}), \tag{1.4b}$$

$$\sigma(\rightleftarrows) = \sigma(+-) = \sigma_{0\rm tot} - |{\rm P}_{\rm B}^{+}{\rm P}_{\rm T}^{-}|\ (\sigma_{1\rm tot} + \sigma_{2\rm tot}), \tag{1.4c}$$

$$\sigma(\leftleftarrows) = \sigma(--) = \sigma_{0\rm tot} + |{\rm P}_{\rm B}^{-}{\rm P}_{\rm T}^{-}|\ (\sigma_{1\rm tot} + \sigma_{2\rm tot}). \tag{1.4d}$$

The signs in brackets correspond to the $\mathbf{P}_{\rm B}$ and $\mathbf{P}_{\rm T}$ directions with respect to $\mathbf{k}$, in this order. In principle, an arbitrary pair of one parallel and one antiparallel beam and target polarization directions determines $\Delta\sigma_{\rm L}$. By using two independent pairs, we remove an instrumental asymmetry term (IA).

Below the neutron beam and the proton target are considered. Since the $\mathbf{P}_{\rm B}$ direction at the Synchrophasotron could be reversed every cycle of the accelerator, it is preferable to calculate $\Delta\sigma_{\rm L}$ from the pairs ($\rightrightarrows$), ($\leftrightarrows$), and ($\rightleftarrows$), ($\leftleftarrows$), measured with the same $\mathbf{P}_{\rm T}$ orientation. It helps to avoid long-time efficiency

fluctuations of the neutron detectors. The spin-averaged term $\sigma_{0\mathrm{tot}}$ drops out when taking the difference, and one obtains

$$-\Delta\sigma_{\mathrm{L}}(\mathrm{P}_{\mathrm{T}}^{+}) \;=\; 2\,(\sigma_{1\mathrm{tot}}+\sigma_{2\mathrm{tot}})^{+} = \frac{2\,[\sigma(\rightrightarrows)-\sigma(\leftrightarrows)]}{(|\mathrm{P}_{\mathrm{B}}^{+}|+|\mathrm{P}_{\mathrm{B}}^{-}|)\;|\mathrm{P}_{\mathrm{T}}^{+}|}, \qquad (1.5a)$$

$$-\Delta\sigma_{\mathrm{L}}(\mathrm{P}_{\mathrm{T}}^{-}) \;=\; 2\,(\sigma_{1\mathrm{tot}}+\sigma_{2\mathrm{tot}})^{-} = \frac{2\,[\sigma(\leftrightarrows)-\sigma(\rightleftarrows)]}{(|\mathrm{P}_{\mathrm{B}}^{+}|+|\mathrm{P}_{\mathrm{B}}^{-}|)\;|\mathrm{P}_{\mathrm{T}}^{-}|}. \qquad (1.5b)$$

Measured differences $-\Delta\sigma_{\mathrm{L}}$, i.e. the asymmetry effect between the total cross sections for parallel and antiparallel orientations of the beam and target polarization, are proportional to the mean value of the beam polarization $|\mathrm{P}_{\mathrm{T}}^{+}|$ and $|\mathrm{P}_{\mathrm{T}}^{-}|$

$$|\mathrm{P}_{\mathrm{B}}| = \frac{1}{2}(|\mathrm{P}_{\mathrm{B}}^{+}|+|\mathrm{P}_{\mathrm{B}}^{-}|). \qquad (1.6)$$

The $|\mathrm{P}_{\mathrm{B}}|$ value is well known as functions of time, because it continuously monitored by a beam polarimeter.

Each of relations (1.5a) and (1.5b) contains a hidden contribution from the instrumental asymmetry IA, caused mainly by a misalignment of the neutron detector counters (see below). The value of IA is given as

$$\mathrm{IA} \;= \frac{1}{2}[\Delta\sigma_{\mathrm{L}}(\mathrm{P}_{\mathrm{T}}^{+}) - \Delta\sigma_{\mathrm{L}}(\mathrm{P}_{\mathrm{T}}^{-})]. \qquad (1.7)$$

The IA disappears, giving the final results as a simple average

$$\Delta\sigma_{\mathrm{L}} = \frac{1}{2}[\Delta\sigma_{\mathrm{L}}(\mathrm{P}_{\mathrm{T}}^{+}) + \Delta\sigma_{\mathrm{L}}(\mathrm{P}_{\mathrm{T}}^{-})]. \qquad (1.8)$$

$\sigma_{0\mathrm{tot}}$, $\Delta\sigma_{\mathrm{T}}$ and $\Delta\sigma_{\mathrm{L}}$ are linearly related to the imaginary parts of the three independent forward scattering invariant amplitudes $a+b$, c and d [27] via optical theorems:

$$\sigma_{0\mathrm{tot}} = (2\pi/K)\;\Im m\;[a(0)+b(0)], \qquad (1.9)$$

$$-\Delta\sigma_{\mathrm{T}} = (4\pi/K)\;\Im m\;[c(0)+d(0)], \qquad (1.10)$$

$$-\Delta\sigma_{\mathrm{L}} = (4\pi/K)\;\Im m\;[c(0)-d(0)], \qquad (1.11)$$

where K is the CM momentum of the incident nucleon. The amplitudes in Eqs. (2.9) to (2.11) satisfy: $a(0)-b(0) = c(0)+d(0)$. The optical theorems always provide the absolute amplitudes, as discussed in [30, 31, 32].

Using the measured $\Delta\sigma(np)$ values and the existing $\Delta\sigma(pp)$ data at the same energy, one can deduce $\Delta\sigma_{\mathrm{L,T}}$ $(I=0)$ as

$$\Delta\sigma_{\mathrm{L,T}}(I=0) = 2\Delta\sigma_{\mathrm{L,T}}(np) - \Delta\sigma_{\mathrm{L,T}}(pp). \qquad (1.12)$$

2. METHOD OF MEASUREMENT

In the transmission experiment we have measured the part of the incident beam particles which remains in the beam after its passage through the target. For the experiments with incident neutrons this measurement is always relative. The neutron beam has a circular profile, formed by the preceding beam collimators. Out of the collimator diameter the neutron flux is considered to be zero. The neutron beam intensity is monitored by neutron beam monitors, placed upstream from the target. The target material consists of small beads inserted in a cylindrical container of the circular profile. The container covers the beam spot and its horizontal axis coincides with the beam axis. The transmission detectors, downstream from the target, are larger than the beam dimensions. Any unscattered beam particle is detected with the same probability.

If $N_{\rm in}$ is the number of neutrons entering the target and $N_{\rm out}$ is the number of neutrons transmitted in a counter array of solid angle Ω, then the total cross section $\sigma(\Omega)$ is related to measured quantities

$$\frac{N_{\rm out}}{N_{\rm in}} = \exp\bigl(-\sigma(\Omega) \times n \times d\bigr), \tag{2.1}$$

where n is the number of all target atoms per cm^3, d is the target length and $N_{\rm out}/N_{\rm in}$ is the simple transmission ratio. The number of counts of the beam monitor M and of the transmission counter T depends on the efficiency of each detector, i.e. $M = N_{\rm in} \times \eta(M)$ and $T = N_{\rm out} \times \eta(T)$. The extrapolation of $\sigma(\Omega)$ towards $\Omega = 0$ gives the unpolarized total cross section $\sigma_{0\rm tot}$.

In the $\Delta\sigma_{\rm L}(\Omega)$ measurements with a completely filled target, only the number of polarizable hydrogen atoms $n_{\rm H}$ is important, because the $\sigma_{\rm tot}$ depends on the polarizations $\rm P_B^{\pm}$ and $\rm P_T^{\pm}$ as shown in Eqs. (1.4). If one sums over the events taken with one fixed target polarizations $\rm P_T^+$ or $\rm P_T^-$ and using Eq. (1.5a) or (1.5b), the double transmission ratios of the measurements with the averaged $\rm P_B$ from Eq. (2.6) for the two $\mathbf{P}_{\rm T}$ directions become

$$\frac{N_{\rm out}(++)/N_{\rm in}(++)}{N_{\rm out}(-+)/N_{\rm in}(-+)} = \exp\ (-\Delta\sigma_{\rm L}(\Omega)\ |{\rm P_B}\ {\rm P_T^+}|\ n_{\rm H}\ d), \tag{2.2a}$$

$$\frac{N_{\rm out}(--)/N_{\rm in}(--)}{N_{\rm out}(+-)/N_{\rm in}(+-)} = \exp\ (-\Delta\sigma_{\rm L}(\Omega)\ |{\rm P_B}\ {\rm P_T^-}|\ n_{\rm H}\ d)\ . \tag{2.2b}$$

We use here the notation of Eqs. (1.4).

Thus the neutron detector efficiencies drop out. Further we put $N = N_{\rm out}/N_{\rm in}$ depending on $\mathbf{P}_{\rm B}$ and $\mathbf{P}_{\rm T}$ combination and Eqs. (2.3) provide

$$-\Delta\sigma_{\rm L}(\Omega, {\rm P_T^+}) = \frac{1}{|{\rm P_B}\ {\rm P_T}^+|\ n_{\rm H}\ d} \times \ln\ \left(\frac{N(++)}{N(-+)}\right), \tag{2.3a}$$

$$-\Delta\sigma_{\rm L}(\Omega, {\rm P_T^-}) = \frac{1}{|{\rm P_B}\ {\rm P_T}^-|\ n_{\rm H}\ d} \times \ln\ \left(\frac{N(--)}{N(+-)}\right). \tag{2.3b}$$

A systematical uncertainty of $-\Delta\sigma_{\rm L}$ value is mainly caused by the errors in the $|{\rm P_B}|$, $|{\rm P_T}|$ and $n_{\rm H}$. A statistical error of $-\Delta\sigma_{\rm L}$ is given by the formula

$$\delta_{\rm stat} = \frac{1}{|{\rm P_B}\ {\rm P_T}|\ n_{\rm H}\ d} \times \sqrt{\frac{1}{M^+} + \frac{1}{M^-} + \frac{1}{T^+} + \frac{1}{T^-}}\ , \qquad (2.4)$$

where M^+, M^- and T^+, T^- are the statictics for monitor and transmission neutron detectors with the ${\rm P_B}^+$ and ${\rm P_B^-}$ neutron beam polarizations, respectively.

If $\Omega \to 0$, we obtain $\Delta\sigma_{\rm L}(\Omega) \to \Delta\sigma_{\rm L}$.

For the np transmission measurement we may neglect the extrapolation of $\Delta\sigma_{\rm L}(\Omega)$ towards $\Omega = 0$ due to the small sizes of detectors [3, 4, 6, 5]. The Saclay–Geneva (SG) PSA [31] at 1.1 GeV shows that for the angles covered by our detectors the resulting $-\Delta\sigma_{\rm L}$ value decreases by 0.04 mb, if we neglect the extrapolation procedure.

The ratio of $n_{\rm H}$ to other target nuclei depends on the target material. The presence of carbon in the PPT beads adds the term $\sigma_{\rm tot}(C)$ in Eqs. (1.4). This term is spin-independent and its contribution drops out in differences (1.5). The same occurs for ^{16}O and ^{4}He in the target and for the cryogenic envelopes.

However, there are small effects from ^{13}C and ^{3}He, which may be slightly polarized. The global contribution was estimated to be $\pm\ 0.3\,\%$ in Refs. [3, 4].

3. EXPERIMENTAL SET-UP

The $\Delta\sigma_{\rm L}(np)$ experimental set-up was in detail described in our previous publications [3–6]. Here we mention briefly essential items, which are important for the data analysis and results, as well as the items concerning modifications and improvements of the apparatus and of the experimental conditions.

Figure 1 shows the both polarized deuteron and polarized free neutron beam lines [11], the two polarimeters [33, 34], the beryllium target (BT) for neutron production, the collimators C1–C4, the spin rotation magnet (SRM), PPT [8, 9], the monitors M1, M2 of neutron beam intensity, transmission detectors T1, T2, T3 and the detectors NP for neutron beam profile monitoring. The associated electronics was described in [3, 4]. The data acquisition system is based on CAMAC parallel branch highway controlled by IBM PC with the branch driver [12] finished off by one of the authors. The on-line program in Pascal works under DOS.

Accelerated deuterons were extracted at the beam momenta p_d of 4.29, 4.93, 5.36 and 5.57 GeV/c, which were known with a sufficient accuracy of $\approx \pm 1\%$. The average intensity of the primary polarized deuteron beam was $\approx 2 \cdot 10^9$ d/cycle. It was continuously monitored by means of two calibrated ionization chambers placed in the two focal points upstream the neutron production target BT.

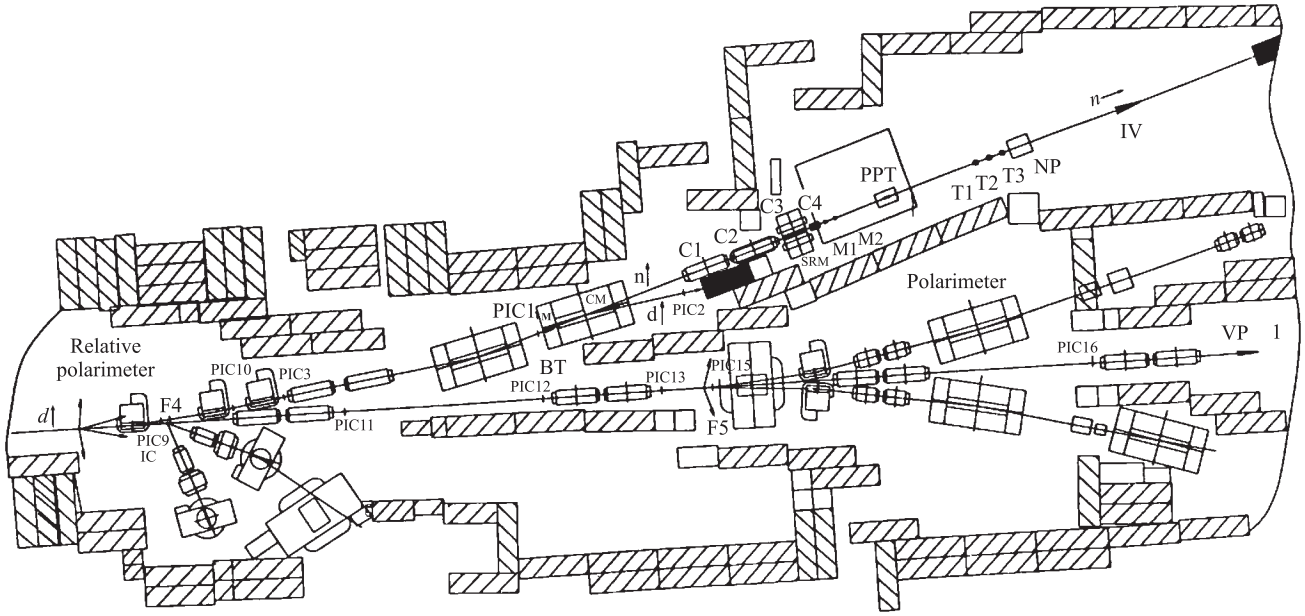

Fig. 1. Experimental set-up for the $\Delta\sigma_{\rm L}(np)$ measurement. Layout of the set-up in the Experimental Hall. VP1 — beam line of extracted, vector polarized deuterons with $\mathbf{P}_{\rm B}(d)$ oriented along the vertical direction $d(\uparrow)$; 1V — beam line to generate and form the polarized neutron beam, $n(\uparrow)$ — neutrons polarized vertically, $n(\rightarrow)$ — neutrons polarized longitudinally; BT — beryllium target for neutron production; IC — ionization chamber for monitoring the deuteron beam intensity; PIC 1–3, 9–16 — multiwire proportional/ionization chambers to measure the deuteron beam profiles; SM — sweeping magnet; C1–C4 — set of neutron beam collimators; SRM — neutron spin rotating dipole; PPT — polarized proton target; and NP — neutron beam profilometer

The beam of free quasi-monochromatic neutrons, polarized along the vertical direction, was obtained by break-up at 0° of vector polarized deuterons in BT. Neglecting the BT thickness, neutrons have a laboratory momentum $p_n = p_d/2$ with a momentum spread of FWHM $\simeq 5\%$ [35]. This corresponds to the neutron beam energies $T_{\rm kin}(n)$ of 1.40, 1.70, 1.90 and 2.00 GeV, respectively. BT contains 20 cm Be with the cross section of $8 \times 8\,{\rm cm}^2$. Energy losses of deuterons during their passage through air, foils in vacuum tubes of the beam transport line and the BT matter provided the decrease of the deuteron beam energy by 20 MeV in the BT center and the mean neutron energy decreases by 10 MeV [3, 5]. For the $\Delta\sigma_{\rm L}$ results the energies and laboratory momenta in the BT center are quoted, for the beam polarization measurements the extracted beam energies have been used.

After the deuteron break-up, the resulting neutrons and protons have the same values and directions of the polarizations, $\mathbf{P}_{\rm B}(n)$ and $\mathbf{P}_{\rm B}(p)$, respectively, as the vector polarization $\mathbf{P}_{\rm B}(d)$ of the incident deuteron beam [36, 37].

In our previous experiments [3, 4, 5, 6] the deuteron beam polarization was determined by two independent asymmetry measurements, either for the dp elastic, or for the pp quasielastic reactions. In the first case, the four-arm beam line polarimeter [33] was used and deuterons, scattered on the liquid hydrogen target, were analyzed by the magnetic field. This polarimeter worked in the primary deuteron beam line. It accurately determined the elastic dp scattering asymmetry at $T_{\rm kin}(d)$ = 1.60 GeV, where the analyzing power of this reaction is well known [38]. In principle, the $\mathbf{P}_{\rm B}(d)$ needs to be determined at one energy value only, since no deuteron depolarizing resonance at the Synchrophasotron exists [33]. On the other hand, the measurement requires to change the deuteron energy and to extract deuterons in another beam line, which is a time-consuming operation. For this reason the dp polarimeter was not used in the 2001 run. In Refs. [5, 6] we obtained an average for positive and negative signs of the vector polarization $|{\rm P}_{\rm B}(d)| = 0.524 \pm 0.010({\rm stat.}) \pm$ $\pm 0.010({\rm syst.})$.

Another four-arm beam polarimeter [34] with small acceptance of $7.1 \cdot 10^{-4}$ sr continuously monitored $\mathbf{P}_{\rm B}(p)$ value during the data acquisition. The deuteron beam, considered as a beam of quasifree protons and neutrons, was scattered on CH_2 target at 14° lab. This polarimeter measured the pp left-right asymmetry on hydrogen and carbon at $T_{\rm kin}(p) = T_{\rm kin}(d)/2$ and the pC asymmetry was subtracted. The polarimeter was calibrated and improved [39, 40]. Average value $|{\rm P}_{\rm B}(p)| \approx |{\rm P}_{\rm B}(d)| = 1/2(|{\rm P}_{\rm B}^+| + |{\rm P}_{\rm B}^-|)$ of deuteron beam polarization was continiously measured by this device during the 2001 data taking run. These $|{\rm P}_{\rm B}(d)|$ values were taken into account for the data treatment. The weighted average $|{\rm P}_{\rm B}(d)|$ over the 2001 run is $|{\rm P}_{\rm B}(d)| = 0.528 \pm$ $0.004({\rm stat.}) \pm 0.008({\rm syst.})$, and agrees with the previous dp polarimeter results very well.

The dimensions and positions of the iron and brass collimators C1–C4 (Fig. 1) were as described in [3, 4]. The accurate measurements of the collimated neutron beam profiles were performed in a dedicated run, using nuclear emulsions. During the data acquisition, the position and $X-Y$ profiles were monitored by the neutron beam profile monitor NP. It was equipped by multiwire proportional chambers and placed close downstream from the last transmission detector.

In order to change the vertical orientation of the neutron beam polarization to the longitudinal direction, a spin-rotating magnet (SRM) was used. The SRM magnetic field map was accurately measured and the value of magnetic field was continuously monitored by a Hall probe. The uncertainty of the magnetic field integral within the neutron beam path area may provide a small additional systematic error of $\pm 0.2\%$.

The frozen-spin polarized proton target reconstructed to the movable device [8, 9, 13] was used. The target material was 1-penthanol ($C_5H_{12}O$ + 5% H_2O) with a paramagnetic Cr^V impurity (EHBA) having the spin concentration of $7 \cdot 10^{19}\,\mathrm{cm}^{-3}$. The penthanol beads were loaded in a thin-wall teflon container 200 mm long and 30 mm in diameter, placed inside the dilution refrigerator. The weight of the penthanol beads was (80.1 $\pm$ 0.05) g and the total number of polarizable hydrogen atoms on the beam neutron path is $n_{\mathrm{H}} \times d = (9.14 \pm 0.10)\ 10^{23}\,\mathrm{cm}^{-2}$.

The PPT polarization $\mathbf{P}_{\mathrm{T}}$ was measured using a computer-controlled NMR system. These measurements were carried out during the run at the beginning and at the end of data taking for each sign of the PPT polarization. The negative and positive target proton polarizations were near the values of –0.75 and 0.60, respectively. The relaxation times were more than 5000 for ${\mathrm{P_T}}^-$ and 7000 hours for ${\mathrm{P_T}}^+$. The relative uncertainty of the measured $\mathbf{P}_{\mathrm{T}}$ values has been estimated at $\pm 5\%$. This uncertainty includes the errors of polarization uniformity measurements using the NMR data from three coils placed inside the PPT container along all the target. The current values of the $\mathbf{P}_{\mathrm{T}}$ were taken into account during the accumulated data processing.

The configuration of the two neutron intensity monitors M1 and M2 and of the three transmission detectors T1, T2 and T3 is shown in Fig. 2. Each of the detectors is to be independent of any other. All the units were of the similar design [16] and the electronics systems were identical, as described in [3, 4]. Each unit consisted of a CH_2 converter, 60 mm thick, placed behind a large veto scintillation counter A. The emitted forward charged particles, generated by neutron interactions in the convertor matter, were detected by two counters S1 and S2 in coincidence. The converters and S1, S2 counters for monitors M1 and M2 were 30 mm in diameter and the corresponding elements for the transmission detectors T1, T2 and T3 were 90, 92 and 94 mm, respectively.

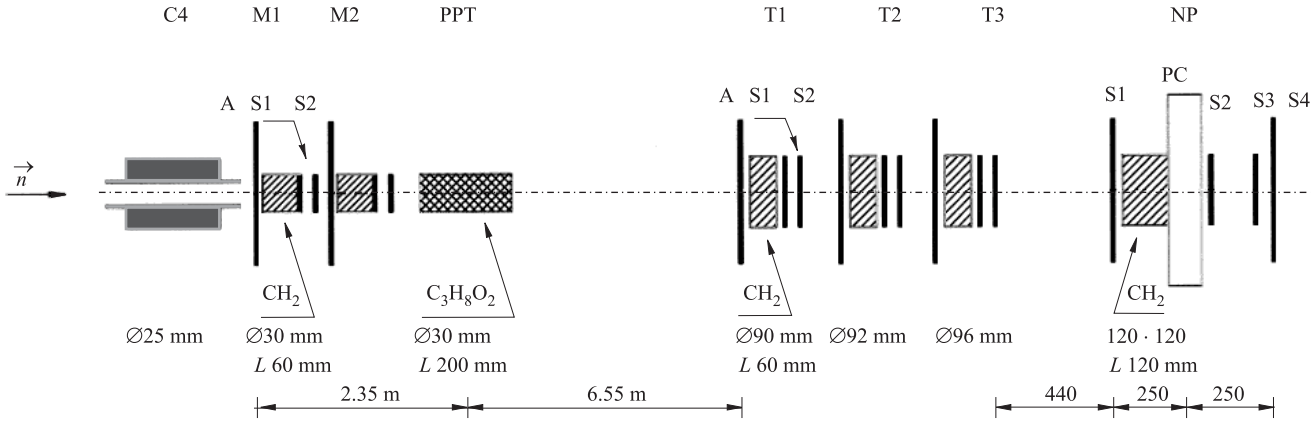

Fig. 2. Experimental set-up for the $\Delta\sigma_{\mathrm{L}}(np)$ measurement. Layout of the detectors for the neutron transmission measurement. C4 — last neutron beam collimator, 25 mm in diameter; M1, M2 — monitor neutron detector modules; PPT — polarized proton target; T1, T2, T3 — neutron transmission detector modules; NP — neutron beam profile monitor; CH_2 — converters; A — anticoincidence scintillation counters; S1–S4 — coincidence scintillation counters; PC — multiwire proportional chambers X, Y

The NP array, also shown in Fig. 2, was similar to the neutron detectors. The two multiwire proportional chambers behind the converter were protected by its own veto A and triggered by the dedicated S1, S2 and S3 counters in coincidence. The used counter array provides very good stability of the detection efficiency. The efficiencies of $\approx 2\%$ for all detectors are practically constant with energy.

The result of $\Delta\sigma_{\rm L}$ is independent of the neutron beam intensity, if the probability of quasi-simultaneous detection of two neutrons in one detector unit may be neglected. The small detection efficiencies decrease the probability for a converted neutron to be accompanied by another quasi-simultaneous converted neutron in the same detector. «Simultaneous» detection is to be understood within the resolution time of a scintillation counter. The probability was estimated from the results obtained with different neutron beam intensities and radiator thicknesses [16, 17]. For the same neutron fluxes, the probability increases quadratically with increasing detector efficiency. At high efficiencies (namely for *pp* transmission experiments) it represents the dominant source of systematic errors. This effect of the «simultaneous» detection of two neutrons in one detector unit, was estimated to be smaller than $2 \cdot 10^{-6}$ in the present experiment.

The misalignment of the detector components or of the entire detectors provide instrumental asymmetry IA. To reach a perfect alignment is beyond the experimental possibility. In the case of misalignment, the asymmetries in each neutron detector depend on the transverse beam polarization components only. For T detectors the misalignment effects are practically independent of the target polarizations [41, 16]. The instrumental asymmetry IA in Eq. (1.7) may be of the same order or larger than the transmission effects and provides the same contributions to each pair of measurements in Eqs. (1.5a) or (1.5b). It is obvious that this effect will be considerably stronger for the $\Delta\sigma_{\rm T}$ measurement, than for the $\Delta\sigma_{\rm L}$ one, where only residual perpendicular $\mathbf{P}_{\rm B}$ components exist. These undesirable components depend on the accuracy of the SRM current setting. As already mentioned, IA cancels out when taking the simple average of results in Eq. (2.8). The results strongly depend on the detector stabilities and their fixed positions over the data acquisition with both $\rm P_T$ signs.

However, there exist small random-like instrumental effects (RLE), provided, e.g. by temperature, magnetic field fluctuations, beam position variations, etc. They affect the stability of set-up elements in an uncontrolled manner. For the final $\Delta\sigma_{\rm L}$ results, uncertainties caused by these effects were taken into account using a special procedure of data treatment (see Sec. 4).

A possible inefficiency of the protection against charged particles by all veto counters may exist. Charged particles in the neutron beam are produced mainly in beam collimators, in CH_2 radiators of all M and T detectors, and in the target. Only a small fraction of the forward protons is polarized. They are

produced in the polarized target by elastic scattering of polarized neutrons on free polarized protons close to $\theta_{\rm CM} = 180^\circ$. For the longitudinally polarized beam and target one obtains a contribution from the spin correlation parameter $A_{00kk}(np)$ [27], which is included in the counting rate asymmetry for the observable $\Delta\sigma_{\rm L}$. This additional asymmetry was calculated in [3, 4] and may provide a $\pm 0.1\%$ systematic error. Let us note that $A_{00kk}(180^\circ,\ np)$ is one of the observables which determine the real parts of the forward scattering amplitudes for the isospin $I = 0$ state. Its measurement is foreseen in our future experiment.

For the measured $\Delta\sigma_{\rm L}$ values, the relative normalization and systematic errors from different sources are summarized as follows:

Beam polarization over the run	$\pm\ 0.9\%$
Target polarization	$\pm\ 5.0\%$
Number of the polarizable hydrogen atoms	$\pm\ 1.1\%$
Polarization of other atoms	$\pm\ 0.3\%$
Magnetic field integral of the neutron spin rotator	$\pm\ 0.2\%$
Inefficiencies of veto counters	$\pm\ 0.1\%$
Total of the relative systematic errors	$\pm\ 5.3\%$
Absolute error due to the extrapolation of results towards 0°	< 0.04 mb

Dedicated tests of the experimental set-up were performed during additional runs with high intensity unpolarized deuteron beams. The unpolarized neutron beam energies were 1.3, 1.4 and 1.5 GeV. We used the same transmission set-up as described above, where PPT was removed and either the liquid hydrogen or carbon targets were inserted in the neutron beam line. Transmission ratios were completed by the corresponding empty target data.

These measurements allowed one to extract the total cross sections $\sigma_{0\rm tot}(np)$ and $\sigma_{0\rm tot}(nC)$. For nC experiment at $T_{\rm kin}(n)$ = 1.5 GeV, the transmission was measured using several carbon targets having different thickness. The obtained results for the three total cross sections are summarized in Table 1.

Table 1. Unpolarized total cross sections for np and nC interactions

$T_{\rm kin}(n)$, GeV	$\sigma_{0\rm tot}(np)$, mb	$\sigma_{0\rm tot}(nC)$, mb
1.30 ± 0.013	41.35 ± 0.66	$-$
1.40 ± 0.014	39.18 ± 0.48	381.5 ± 2.6
1.50 ± 0.015	41.63 ± 0.83	379.6 ± 1.0

Our results are shown in Figs. 3 and 4, where they are compared with existing data, listed in compilations [42, 43, 44] for np and in [45] for nC interactions.

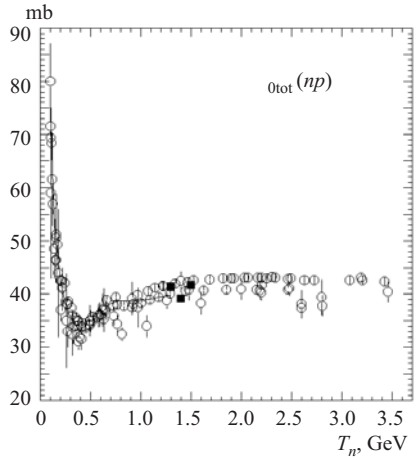

Fig. 3. Energy dependence of the $\sigma_{0\mathrm{tot}}(np)$. The meaning of the symbols: ○ — world data from [42, 43, 44], ■ — this experiment, —— — GW/VPI-PSA [47] (SP03 solution)

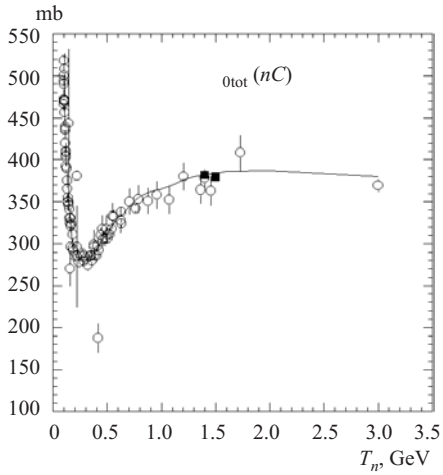

Fig. 4. Energy dependence of the $\sigma_{0\mathrm{tot}}(nC)$. The meaning of the symbols: ○ — world data from [45], ■ — this experiment, —— — [45]

4. DATA ANALYSIS

For each accelerator cycle the following main information was recorded and displayed by the data acquisition system:

• rates of the two calibrated ionization chambers used as primary deuteron beam intensity monitors,

• rates of coincidences and accidental coincidences for the two neutron detectors M1 and M2 used as the intensity monitors of the neutron beam incident on the PPT,

• rates of coincidences and accidental coincidences for the three neutron transmission detectors T1, T2 and T3,

• rates of the left and right arms of the pp beam polarimeter.

At the beginning of the run, statistics at T_{kin} = 1.4 GeV with $\mathrm{P}_{\mathrm{T}}^{+}$ and $\mathrm{P}_{\mathrm{T}}^{-}$ were recorded. Then the data were taken at 1.7, 2.0 GeV and 1.9 GeV with $\mathrm{P}_{\mathrm{T}}^{-}$. Finally, with $\mathrm{P}_{\mathrm{T}}^{+}$ the data were acquired at 1.9, 2.0 and 1.7 GeV.

The recorded data were then analyzed in three steps. In the first step, the data were cleaned of a low-quality information. At first, the «bad» data files

were removed. Then the data files were cleaned of the «bad» cycles with an absence or incorrect sequence of labels of $\mathrm{P_B}$ signs. The number of such «bad» cycles for the cumulated statistics is a few tenths of percent. The data were also cleaned of the cycles with an absence («empty» cycle) or a low level beam intensity and/or with a possible fluctuation of the neutron detector performances. The main part of the rejected cycles ($\sim 5\%$) was caused by the low intensity of neutron beam. Remaining event statistics over the run at a given energy and for each combination of the $\mathbf{P}_\mathrm{B}$ and $\mathbf{P}_\mathrm{T}$ directions were used to determine $\Delta\sigma_\mathrm{L}$ and IA. The transmission ratios from Eqs. (2.3) averaged over the beam and target polarizations are proportional to $\sigma_{0\mathrm{tot}}$(PPT) for all targets elements. The transmission ratios were listed in [5, 6] at three energies and are not shown here, since the conclusions are identical. With decreasing energy $\sigma_{0\mathrm{tot}}$(PPT) slightly decreases. A monotonous decrease of the $\sigma_{0\mathrm{tot}}$(PPT) as a function of the neutron transmission detector distance from the target is also observed, as expected.

The second and third steps of data analysis used the previously selected events. The stabilities of the SRM magnetic field and of the neutron detectors were checked, the parameters of statistical distributions of the $\Delta\sigma_\mathrm{L}$ results for all pairs of the neighbour cycles with $\mathrm{P_B^+}$ and $\mathrm{P_B^-}$ for a sequence of data cycles accumulated over a single run were determined and the final results were obtained. The transmission ratios as functions of time were analyzed for each combination of the individual M and T detectors, at any neutron energy and the $\mathrm{P_T}$ sign. No significant time dependence of checked values and no sizeable deviations from normal distributions were observed.

The $\Delta\sigma_\mathrm{L}$ values over a given run were calculated by two different methods. By the first method, the $\Delta\sigma_\mathrm{L}$ values were obtained using Eqs. (2.4a), (2.4b) and (2.5) for entire statistics of each neutron detector (M1, M2, T1, T2, T3), accumulated over the run. For the second method, first the partial $\Delta\sigma_\mathrm{L}$ values end their statistical errors were calculated from the individual neutron detector statistics for each «pair» of the following cycles with the opposite beam polarizations $\mathrm{P_B^+}$ and $\mathrm{P_B}^-$. The relations (2.4a), (2.4b), (2.5) and the known time-dependent sequence of recorded cycles were used again. Then, obtained partial $\Delta\sigma_\mathrm{L}$ values and their statistical errors for all «pairs» were added using an average weighing. The second method takes into account both the statistical uncertainties and the «random-like» instrumental effects — RLE.

The final results of the data treatment are presented in Table 2. The $-\Delta\sigma_\mathrm{L}(np)$ values at four energies, measured with the individual transmission detectors T1, T2, T3 for both sign of $\mathrm{P_T}$, their half-sums from Eq. (1.8) and half-differences, i.e. the hidden contributions of IA [16] from Eq. (1.7), are listed. The results were obtained using the combined statistics from the two monitors M1 and M2. The T123 value at any energy represents the wieghted average of the three transmission detectors contributions.

Table 2. Measured $-\Delta\sigma_{\rm L}(np)$ values at different neutron beam energies $T_{\rm kin}(n) = T_n$ GeV for the two opposite target polarizations, for the individual transmission detectors (TD) and for the cumulated statistics

T_n	TD	$-\Delta\sigma_{\rm L}(\rm P_T^+)$, mb	$-\Delta\sigma_{\rm L}(\rm P_T^-)$, mb	IA, mb	Average $-\Delta\sigma_{\rm L}$, mb	R
1.39	T1	$+12.14 \pm 3.09$	$+3.33 \pm 2.48$	$+4.41$	$+7.73 \pm 1.98$	1.195
	T2	$+10.83 \pm 3.17$	$+2.92 \pm 2.56$	$+3.95$	$+6.87 \pm 2.04$	1.204
	T3	$+7.73 \pm 3.28$	$+1.23 \pm 2.65$	$+3.25$	$+4.48 \pm 2.11$	1.211
	T123	$+10.32 \pm 1.83$	$+2.54 \pm 1.48$	$+3.69$	$+6.43 \pm 1.18$	1.036
1.69	T1	$+2.53 \pm 2.04$	$+0.68 \pm 1.58$	$+0.92$	$+1.60 \pm 1.29$	1.190
	T2	$+4.51 \pm 2.09$	-1.65 ± 1.62	$+3.08$	$+1.43 \pm 1.32$	1.197
	T3	$+6.08 \pm 2.17$	$+0.86 \pm 1.68$	$+2.61$	$+3.47 \pm 1.37$	1.203
	T123	$+4.30 \pm 1.21$	-0.41 ± 0.94	$+2.17$	$+2.13 \pm 0.77$	1.037
1.89	T1	$+3.47 \pm 2.34$	$+3.08 \pm 2.46$	$+0.20$	$+3.27 \pm 1.70$	1.272
	T2	-0.84 ± 2.41	$+2.40 \pm 2.54$	-1.62	$+0.78 \pm 1.75$	1.284
	T3	$+1.17 \pm 2.49$	$+4.74 \pm 2.63$	-1.78	$+2.96 \pm 1.81$	1.295
	T123	$+1.31 \pm 1.39$	$+3.37 \pm 1.47$	-1.03	$+2.34 \pm 1.01$	1.043
1.99	T1	$+0.76 \pm 2.03$	$+2.87 \pm 1.85$	-1.06	$+1.82 \pm 1.37$	1.222
	T2	-1.47 ± 2.09	$+3.82 \pm 1.90$	-2.64	$+1.17 \pm 1.41$	1.230
	T3	$+0.71 \pm 2.16$	$+2.35 \pm 1.97$	-0.82	$+1.53 \pm 1.46$	1.239
	T123	$+0.0003 \pm 1.21$	$+3.03 \pm 1.10$	-1.51	$+1.51 \pm 0.82$	1.030

The data presented in the table were calculated using the procedure of average weighing of the results for each pair of the neighbour cycles from the sequence of all accumulated data cycles with $\rm P_B^+$ and $\rm P_B^-$ beam polarizations. Therefore the errors quoted take into account both the statistical uncertainties and the «random-like» instrumental effects. Since both the IA and the average $-\Delta\sigma_{\rm L}(np)$ values have the same errors, they are indicated for the $-\Delta\sigma_{\rm L}(np)$ values only.

The $-\Delta\sigma_{\rm L}$ values and their experimental errors presented in Table 2 have been calculated by the second («pair») method. In order to estimate the RLE contribution to the experimental error we calculated the ratio

$$R = \delta_{\text{«pair»}}/\delta_{\rm stat} \geqslant 1, \tag{4.1}$$

where the $\delta_{\text{«pair»}}$ is the error obtained by the second method and $\delta_{\rm stat}$ is the error obtained by the first one.

The value of $R = 1$ occurs if no RLE exists and it increases with increasing RLE. In our experiment the errors of the final results obtained by the «pair» method exceed the statistical errors obtained from Eq. (2.5) by $\sim 4\%$ (see last column in Table 2).

As can be seen from Table 2, the IA values at 1.39 and 1.69 GeV are positive, whereas at 1.89 and 1.99 GeV they are mostly negative. Since the elements of the neutron detectors were not moved during the run, we assume that the residual perpendicular components in $\mathbf{P}_{\mathrm{B}}$ were opposite.

5. RESULTS AND DISCUSSION

The final $-\Delta\sigma_{\mathrm{L}}(np)$ values are presented in Table 3 and shown in Fig. 5. Statistical and systematic errors are taken into account. Total errors are the quadratic sums of experimental and systematic uncertainties.

Table 3. Final $-\Delta\sigma_{\mathrm{L}}(np)$ results. Total errors are quadratic sums of the experimental and systematic errors. Laboratory kinetic energies and momenta of the neutron beam in the production target center are given

$T_{\mathrm{kin}}(n)$, GeV	$p_{\mathrm{lab}}(n)$, GeV/c	$-\Delta\sigma_{\mathrm{L}}(np)$, mb	Exp. error, mb	Syst. error, mb	Total error, mb
1.39	2.13	$+6.43$	±1.18	±0.34	±1.23
1.69	2.46	$+2.13$	±0.77	±0.11	±0.78
1.89	2.67	$+2.34$	±1.01	±0.12	±1.02
1.99	2.77	$+1.51$	±0.82	±0.08	±0.82

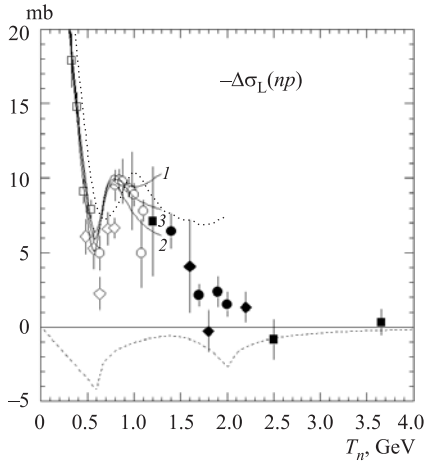

Fig. 5. Energy dependence of the $-\Delta\sigma_{\mathrm{L}}(np)$. The meaning of the symbols: ● — this experiment, ■ — JINR [3, 4], ◆ — JINR [5, 6], □ — PSI [19], ◇ — LAMPF [20], ○ — Saturne II [16, 17], —— — ED GW/VPI PSA [46, 47] (*1* — FA95 solution, *2* — SP99 solution and *3* — SP03 solution), $\cdots$ — meson-exchange model [51], - - - - — contribution from nonperturbative QCD interaction induced by instantons [3, 4, 6]

The results from Refs. [3–6] together with the existing $-\Delta\sigma_{\mathrm{L}}(np)$ data [16, 17, 19, 20], obtained with free polarized neutrons below 1.1 GeV, are also plotted in Fig. 5. In [5] we added the TUNL point at 19.7 MeV [25] and the PSI point

at 66 MeV [21], in order to show the $-\Delta\sigma_{\rm L}(np)$ energy dependence and existing structure at low energies. This structure (not shown here) was described by the energy dependent (ED) GW/VPI PSA (solution SP99) [46] and is described again in the recent solution SP03 [47]. In the present paper we discuss mainly the energy dependence over the high energy region.

The new results agree with our previous data, confirming a fast decrease above 1.1 GeV, and suggest a minimum or a shoulder in the vicinity of 1.8 GeV. The quasielastic pn data from Ref. [15] (not shown here) are in good agreement with the Dubna results. The solid curves represent the evolution of the PSA fits of $-\Delta\sigma_{\rm L}(np)$ — FA95, SP99 and SP03 GW/VPI PSA solutions [46, 47] below 1.3 GeV. Above 0.6 GeV the fits are only in qualitative agreement with the measured values.

From Eq. (1.12) can be deduced $-\Delta\sigma_{\rm L}(I=0)$, using the obtained $-\Delta\sigma_{\rm L}(np)$ results and the corresponding pp values at the same energies. In order to determine $-\Delta\sigma_{\rm L}(pp)$, we have used different sources:

• Calculations using the energy dependent (ED) GW/VPI PSA [47] (solution SP03).

• Linear interpolation of the fixed energy (FE) GW/VPI PSA [47] results, using the solutions at 1.275, 1.50, 1.70, 1.80, 1.95, and 2.025 GeV.

• Linear interpolation of the FE Saclay–Geneva (SG) PSA results [31], using the solutions at 1.3, 1.6, 1.8, 2.1 GeV.

• Interpolation of the pp experimental data measured at ANL–ZGS [48, 49] and Saturne II [50] in the vicinity of energy values for the obtained $-\Delta\sigma_{\rm L}(np)$ data.

The four calculated pp data sets are listed in the upper part of Table 4. Let us note that from ED GW/VPI PSA no errors could be calculated and in FE GW/VPI PSA they are obviously overestimated. SG PSA calculate errors using the error matrix, which are compatible with those obtained by the direct interpolation of neighbourhood measured values.

The results of $-\Delta\sigma_{\rm L}(I=0)$, using the four sets of pp values are given in the bottom part of Table 4. We have added the SG PSA errors to the ED GW/VPI pp predictions. The results at each energy agree within the errors. Since, in general, the pp data are accurate, the $-\Delta\sigma_{\rm L}(I=0)$ values have roughly two times larger errors than the np results. For this reason, an improved accuracy of np measurements is important.

New $-\Delta\sigma_{\rm L}(I=0)$ results, calculated with ED GW/VPI pp values are plotted in Fig. 6, together with other existing data in a large energy interval. The solid curves were calculated from np and pp ED GW/VPI PSA ([46, 47] solutions FA95, SP99, SP03) predictions below 1.3 GeV. The PSA fits described inaccurately the data starting 0.5 GeV. In addition, for comparison, the energy dependence of isovector part $-\Delta\sigma_{\rm L}(I=1)$, calculated from ED GW/VPI (solution SP03) is shown by dotted line.

Table 4. The upper part: $-\Delta\sigma_{\rm L}(pp)$ values deduced from the four sources. The lower part: Four sets of $-\Delta\sigma_{\rm L}(I=0)$ results, calculated from the present np data and corresponding pp values

$T_{\rm kin}$, GeV	$-\Delta\sigma_{\rm L}(pp)$, mb ED GW/VPI	$-\Delta\sigma_{\rm L}(pp)$, mb FE GW/VPI	$-\Delta\sigma_{\rm L}(pp)$, mb FE SG	$-\Delta\sigma_{\rm L}(pp)$, mb data interpol.
1.39	+7.83	$+7.73 \pm 2.13$	$+7.82 \pm 0.30$	$+6.45 \pm 0.53$
1.69	+4.17	$+4.14 \pm 1.71$	$+4.35 \pm 0.30$	$+3.78 \pm 0.30$
1.89	+2.60	$+1.87 \pm 2.27$	$+3.09 \pm 0.30$	$+2.77 \pm 0.18$
1.99	+2.07	$+0.44 \pm 2.21$	$+2.82 \pm 0.20$	$+2.20 \pm 0.18$
$T_{\rm kin}$, GeV	$-\Delta\sigma_{\rm L}(I=0)$, mb	$-\Delta\sigma_{\rm L}(I=0)$, mb	$-\Delta\sigma_{\rm L}(I=0)$, mb	$-\Delta\sigma_{\rm L}(I=0)$, mb
1.39	$+5.03 \pm 2.38$	$+5.13 \pm 3.18$	$+5.04 \pm 2.38$	$+6.43 \pm 2.41$
1.69	$+0.09 \pm 1.58$	$+0.12 \pm 2.29$	-0.09 ± 1.58	$+0.18 \pm 1.58$
1.89	$+2.09 \pm 2.05$	$+2.82 \pm 3.04$	$+1.60 \pm 2.05$	$+1.92 \pm 2.03$
1.99	$+0.95 \pm 1.64$	$+2.59 \pm 2.75$	$+0.21 \pm 1.64$	$+0.82 \pm 1.64$

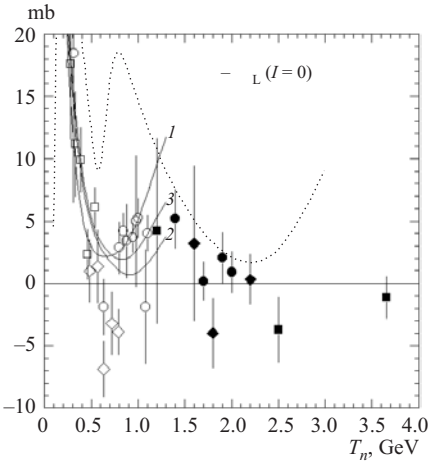

Fig. 6. Energy dependence of the $-\Delta\sigma_{\rm L}(I=0)$ calculated from measured np data and the corresponding pp values from [47] (solution SP03). The np data at the same energies as in Fig. 5 are used and the $I=0$ results are denoted by the same symbols. The solid curves are the $I=0$ dependences calculated from the common np and pp GW/VPI-PSA [46, 47] (*1* — FA95 solution, *2* — SP99 solution and *3* — SP03 solution). For comparison, the $-\Delta\sigma_{\rm L}(I=1)$ dependence from GW/VPI-PSA [47] (solution SP03) is shown by the dotted curve

The new results agree again with our previous data and confirm a plateau around 1.4 GeV followed by a fast decrease and suggest a minimum in the vicinity of 1.8 GeV. The $-\Delta\sigma_{\rm L}(I=0)$ values deduced from the quasielastic pn data [15] above 1 GeV (not shown) are in good agreement with the present results.

Some dynamic models predicted the $-\Delta\sigma_{\rm L,T}$ energy behaviour for np and pp interactions. Below 2.0 GeV, a usual meson exchange theory of NN scat-

tering [51] gives the $-\Delta\sigma_{\rm L}(np)$ energy dependence as shown by the dotted curve in Fig. 5. It can be seen that this model provides only a qualitative description at low energies and disagrees considerably with the data above 1 GeV.

The articles [3, 4, 6] discussed the model of a nonperturbative flavour-dependent interaction between quarks, induced by a strong fluctuation of vacuum gluon fields, i.e. instantons. Estimation of such nonperturbative QCD contribution to the $-\Delta\sigma_{\rm L}(np)$ energy behaviour is shown in Fig.5 by dashed line. One can see that this prediction disagrees with the experimental data.

The investigated energy region corresponds to a possible generation of heavy dibaryons with masses $M > 2.4\,\mathrm{GeV}$ (see [52]). For example, model [53, 54] predicts the formation of a heavy dibaryon state with a color octet–octet structure.

The possible manifestation of exotic dibaryons in the energy dependence of different pp and np observables was predicted by another model [55, 56, 57, 58, 59]. The authors used the Cloudy Bag Model and an R-matrix connection to the long-range meson-exchange force region with the short-range region of asymptotically free quarks. This hybrid model gives the lowest lying exotic six-quark configurations in the isosinglet and the spin-triplet state $^3\mathrm{S}_1$ with the mass $M = 2.63\,\mathrm{GeV}$ ($T_{\rm kin}(n) = 1.81\,\mathrm{GeV}$). This is close to the energy where a minimum is suggested by the energy dependence of our results.

For the $I = 0$ state, the $^3\mathrm{S}_1$ partial wave is expected to be predominant. Since $-\Delta\sigma_{\rm T}$ for arbitrary isospin state contains no uncoupled spin-triplet state, a possible dibaryon resonance effect in $^3\mathrm{S}_1$ may be less diluted. The measurement of $-\Delta\sigma_{\rm T}$ observable for np interaction and deducing from these data the $-\Delta\sigma_{\rm T}(I = 0)$ values may provide a significant more sensitive check of possible manifestation of the predicted dybaryon. Moreover, in the difference of both quantities the spin-singlet contributions vanish. For this reason, the more detailed and accurate measurements of energy dependences of $-\Delta\sigma_{\rm L}(np)$ and $-\Delta\sigma_{\rm T}(np)$ in vinicity of $T_n = 1.8\,\mathrm{GeV}$ are important.

The $I = 0$ spin-dependent total cross sections represent a considerable advantage to study possible resonances. This is in contrast with the $I = 1$ system where the lowest lying exotic six-quark configuration corresponds to the spin-singlet state $^1\mathrm{S}_0$ [59]. This state is not dominant and it is hard to separate it in the forward direction.

The three optical theorems determine the imaginary parts of the nonvanishing forward amplitudes, as shown in Eqs. (2.9) to (2.11). Extrema in $I = 0$ amplitudes or in their combinations dominated by the spin-triplet states will be a necessary condition for the predicted resonance. The sufficient condition may be provided by real parts. For np scattering they can be determined by measurements of observables in the experimentally accessible backward direction, as was shown in [32].

CONCLUSIONS

New $-\Delta\sigma_{\rm L}(np)$ results, obtained in the transmission experiment, complete in the main the measurement of energy dependence at the Dubna Synchrophasotron region. Measured $-\Delta\sigma_{\rm L}(np)$ values are in accordance with the existing data at lower energies. The $-\Delta\sigma_{\rm L}(np)$ energy dependence shows a fast decrease to zero above 1.1 GeV and a possible structure around 1.8 GeV. Values of the $I = 0$ part of $\Delta\sigma_{\rm L}$ are also presented. The data are compared with model predictions and with the PSA fits.

The $-\Delta\sigma_{\rm L}(I = 0)$ quantities, deduced from the measured $\Delta\sigma_{\rm L}(np)$ values and the existing $-\Delta\sigma_{\rm L}(pp)$ data, are also presented. They indicate a plateau or a weak maximum around 1.4 GeV, followed by a rapid decrease with energy and by a minimum around 1.8 GeV.

The obtained results are compared with the dynamic model predictions and with the recent ED GW/VPI-PSA fit. The necessity of more detailed and accurate $-\Delta\sigma_{\rm L}(np)$ measurements around 1.8 GeV and new $-\Delta\sigma_{\rm T}(np)$ data in the kinetic energy region above 1.1 GeV is emphasized.

Acknowledgements. The authors are grateful to the Synchrophasotron staff and all the scientific and engineering groups and individuals who took part and helped us during the $-\Delta\sigma_{\rm L}$ measurements preparation, data taking, and data analysis. The authors also thank the JINR, JINR VBLHE and DLNP Directorates for these investigations support. For the last two years this work was supported in part by the Russian Foundation for Basic Research (Grant No. 02-02-17129).

REFERENCES

1. *Ball J., et al.* // Proc. of the International Workshop «Dubna Deuteron-91». JINR, E2-92-25. Dubna, 1992. P. 12.
2. *Chernykh E. et al.* // Proc. of the International Workshop «Dubna Deuteron-93». JINR, E2-94-95. Dubna, 1994. P. 185;
   Proc. of the V Workshop on High Energy Spin Physics. Protvino, 20–24 September 1993. Protvino, 1994. P. 478.
3. *Adiasevich B. P. et al.* // Z. Phys. C. 1996. V. 71. P. 65.
4. *Sharov V. I. et al.* // JINR Rapid Commun. 1996. No. 3[77]. P. 13.
5. *Sharov V. I. et al.* // Eur. Phys. J. C. 2000. V. 13. P. 255.
6. *Sharov V. I. et al.* // JINR Rapid Commun. 1999. No. 4[96]. P. 17.
7. *Lehar F. et al.* // Nucl. Instr. Meth. A. 1995. V. 356. P. 58.
8. *Bazhanov N. A. et al.* // Nucl. Instr. Meth. A. 1996. V. 372. P. 349.

9. *Bazhanov N. A., et al.* // Nucl. Instr. Meth. A. 1998. V. 402. P. 484.

10. *Issinsky I. B. et al.* // Acta Physica Polonica B. 1994. V. 25. P. 673.

11. *Kirillov A. et al.* Relativistic Polarized Neutrons at the Laboratory of High Energy Physics, JINR. JINR, Preprint E13-96-210. Dubna, 1996.

12. *Gorbunov N. V., Karev A. G.* // Proc. of the XII International Symposium on Nuclear Electronics, September 12–18, Varna, Bulgaria, 1988. JINR, D13-88-938. Dubna, 1989. P. 103.

13. *Anischenko N. G. et al.* // JINR Rapid Commun. 1998. No. 6[92]. P. 49.

14. *Lechanoine-Leluc C., Lehar F.* // Rev. Mod. Phys. 1993. V. 65. P. 47.

15. *Auer I. P. et al.* // Phys. Rev. Lett. 1981. V. 46. P. 1177.

16. *Lehar F. et al.* // Phys. Lett. B. 1987. V. 189. P. 241.

17. *Fontaine J.-M. et al.* // Nucl. Phys. B. 1991. V. 358. P. 297.

18. *Ball J. et al.* // Z. Phys. C. 1994. V. 61. P. 53.

19. *Binz R. et al.* // Nucl. Phys. A. 1991. V. 533. P. 601.

20. *Beddo M. et al.* // Phys. Lett. B. 1991. V. 258. P. 24.

21. *Haffter P. et al.* // Nucl. Phys. A. 1992. V. 548. P. 29.

22. *Brož J. et al.* // Z. Phys. A. 1997. V. 359. P. 23.

23. *Wilburn W. S. et al.* // Phys. Rev. C. 1995. V. 52. P. 2352.

24. *Brož J. et al.* // Z. Phys. A. 1996. V. 354. P. 401.

25. *Walston J. R.* Ph. D. Thesis. North Carolina State University, 1998.

26. *Raichle B. W.* Ph. D. Thesis. North Carolina State University, 1997.

27. *Bystrický J., Lehar F., Winternitz P.* // J. Phys. (Paris). 1978. V. 39. P. 1.

28. *Bilenky S. M., Ryndin R. M.* // Phys. Lett. 1963. V. 6. P. 217.

29. *Phillips R. J. N.* // Nucl. Phys. 1963. V. 43. P. 413.

30. *Ball J. et al.* // Nuovo Cimento. 1998. V. 111. P. 13.

31. *Bystrický J., Lechanoine-Leluc C., Lehar F.* // Eur. Phys. J. C. 1998. V. 4. P. 607.

32. *Ball J. et al.* // Eur. Phys. J. C. 1998. V. 5. P. 57.

33. *Ableev V. G. et al.* // Nucl. Instr. Meth. A. 1991. V. 306. P. 51.

34. *Azhgirey L. S. et al.* // Pribory i Tekhnika Experimenta. 1997. V. 1. P. 51; Instrum. Exp. Techiques. 1997. V. 40. P. 43.

35. *Ableev V. G. et al.* // Nucl. Phys. A. 1983. V. 393. P. 941; Nucl. Phys. A. 1983. V. 411. P. 514. Eratum.

36. *Cheung E. et al.* // Phys. Lett. B. 1992. V. 284. P. 210.

37. *Nomofilov A. A. et al.* // Phys. Lett. B. 1994. V. 325. P. 327.

38. *Ghazikhanian V. et al.* // Phys. Rev. C. 1991. V. 43. P. 1532.

39. *Azhgirey L. S. et al.* // Part. and Nucl., Letters. 2002. 4[113]. P. 51.

40. *Azhgirey L. S. et al.* // Nucl. Instr. Meth. A. 2003. V. 497. P. 340.

41. *Perrot F. et al.* // Nucl. Phys. B. 1986. V. 278. P. 881.

42. *Barashenkov V. S.* Cross Sections of Interactions of Elementary Particles. Moscow: Science, 1966.

43. *Bystrický J. et al.* Elastic and Charge Exchange Scattering of Elementary Particles. Nucleon–Nucleon and Kaon–Nucleon Scattering. Landolt-Börnstein. New Series. V. 9. Berlin; Heidelberg; N.–Y.: Springer–Verlag, 1980.

44. *Bystrický J., Lehar F.* Nucleon-Nucleon Scattering Data / Ed. H. Behrens, G. Ebel. Fachinformationszentrum Karlsruhe, Nr.11-2, Nr.11-3, 1981.

45. *Barashenkov V. S.* Cross Sections of Interactions of Particles and Nuclei with Nuclei. JINR Dubna, 1993.

46. *Arndt R. A. et al.* // Phys. Rev. C. 1997. V. 56. P. 3005.

47. *Arndt R. A., Strakovsky I. I., Workman R. L.* // Phys. Rev. C. 2000. V. 62. 034005.

48. *Auer I. P. et al.* // Phys. Rev. Lett. 1978. V. 41. P. 354.

49. *Auer I. P. et al.* // Phys. Rev. D. 1986. V. 34. P. 2581.

50. *Bystrický J. et al.* // Phys. Lett. B. 1984. V. 142. P. 141.

51. *Lee T.-S. H.* // Phys. Rev. C. 1984. V. 29. P. 195.

52. *Strakovsky I. I.* // Fiz. Elem. Chast. At. Yadra. 1991. V. 22. P. 615; Sov. J. Part. Nucl. 1991. V. 22. P. 296.

53. *Kopeliovich B. Z., Niedermayer F.* // Zh. Eksp. Teor. Fiz. 1984. V. 87. P. 1121; Sov. Phys. JETP. 1984. V. 60(4). P. 640.

54. *Kopeliovich B. Z.* // Fiz. Elem. Chastits At. Yadra. 1990. V. 21. P. 117; Sov. J. Part. Nucl. 1990. V. 21(1). P. 49.

55. *LaFrance P., Lomon E. L.* // Phys. Rev. D. 1986. V. 34. P. 1341.

56. *Gonzales P., LaFrance P., Lomon E. L.* // Phys. Rev. D. 1987. V. 35. P. 2142.

57. *LaFrance P.* // Can. J. Phys. 1990. V. 68. P. 1194.

58. *Lomon E. L.* // Colloque de Physique (France). 1990. V. 51. C6-363.

59. *LaFrance P., Lomon E. L.* // Proc. of the International Conference «Mesons and Nuclei at Intermediate Energies». Dubna, May 3–7, 1994. Singapore: World Scientific, 1995. P. 97.

Received on June 4, 2004.

Корректор *Т. Е. Попеко*

Подписано в печать 15.07.2004.
Формат 60 × 90/16. Бумага офсетная. Печать офсетная.
Усл. печ. л. 1,68. Уч.-изд. л. 2,37. Тираж 490 экз. Заказ 54527.

Издательский отдел Объединенного института ядерных исследований
141980, г. Дубна, Московская обл., ул. Жолио-Кюри, 6.
E-mail: publish@pds.jinr.ru
www.jinr.ru/publish/